Impact of multiangular information on empirical models to estimate canopy nitrogen concentration in mixed forest

Silvia Huber,[a,b,c] Benjamin Koetz,[d] Achilleas Psomas,[e] Mathias Kneubuehler,[b] Jürg T. Schopfer,[b] Klaus I. Itten,[b] and Niklaus E. Zimmermann[e]

[a] University of Copenhagen, Department of Geography and Geology, Øster Voldgade 10, 1350 Copenhagen, Denmark
sh@geo.ku.dk
[b] University of Zurich, Department of Geography, Remote Sensing Laboratories, Winterthurerstrasse 190, 8057 Zurich, Switzerland
[c] Wageningen University, Centre for Geo-Information, PO Box 47, 6700AA Wageningen, The Netherlands
[d] ESA/ESRIN, Via Galileo Galilei, CP 64, 00044 Frascati (Rome), Italy
[e] Swiss Federal Research Institute WSL, Land Use Dynamics, Zuercherstr. 111, 8903 Birmensdorf, Switzerland

Abstract. Directional effects in remotely sensed reflectance data can influence the retrieval of plant biophysical and biochemical estimates. Previous studies have demonstrated that directional measurements contain added information that may increase the accuracy of estimated plant structural parameters. Because accurate biochemistry mapping is linked to vegetation structure, also models to estimate canopy nitrogen concentration (C_N) may be improved indirectly from using multiangular data. Hyperspectral imagery with five different viewing zenith angles was acquired by the spaceborne CHRIS sensor over a forest study site in Switzerland. Fifteen canopy reflectance spectra corresponding to subplots of field-sampled trees were extracted from the preprocessed CHRIS images and subsequently two-term models were developed by regressing C_N on four datasets comprising either original or continuum-removed reflectances. Consideration is given to the directional sensitivity of the C_N estimation by generating regression models based on various combinations (n=15) of observation angles. The results of this study show that estimating canopy C_N with only nadir data is not optimal irrespective of spectral data processing. Moreover adding multiangular information improves significantly the regression model fits and thus the retrieval of forest canopy biochemistry. These findings support the potential of multiangular Earth observations also for application-oriented ecological monitoring.

Keywords: CHRIS/PROBA, canopy biochemistry, subset selection algorithm, continuum removal.

1 INTRODUCTION

Sun and sensor geometries cause directional effects in remotely sensed reflectance data which may influence the estimates of biophysical and biochemical variables. This complicates the interpretation of remotely sensed data of the same geographic location collected by different instruments at varying spatial scales or sampling times [1, 2]. As a consequence, the bidirectional variability is often considered as noise and its impact on the estimation of plant biochemical and structural variables remains unknown in many cases. Yet, it has been recognized that the reflectance anisotropy is intimately related to the structural properties of the observed surfaces [3, 4]. Hence, a number of studies have investigated how to relate surface anisotropy to surface vegetation structure [5-9]. Some

Received 9 May 2007; accepted 19 Apr 2010; published 7 May 2010 [CCC: 19313195/2010/$25.00]

authors found that the use of directional observations could improve the retrieval of relevant ecological parameters such as leaf area index (LAI) [10], gap fraction and leaf orientation [5, 11], tree cover and tree height [12, 13] or wheat yield maps [14]. It was also shown that the separability of land cover types might improve when using multiangular data [15-17].

So far, little attention has been paid to using directional information for the assessment of biochemical properties even though the ability to accurately derive biochemical estimates from remotely sensed data is limited without accounting for canopy structure, by the complex vertical and horizontal structure of vegetation communities [11]. In other words, with improved information on canopy structure also enhanced biochemical estimates can be indirectly expected [18]. The only study that systematically investigated directional data for chlorophyll content retrieval, albeit from reflectance simulations, was performed by Weiss and co-workers [19]. One of the few studies that used real off-nadir measurements to retrieve chlorophyll content by modeling was conducted by Begiebing et al. [18], though without considering backward scattering reflectances and multiangular information (angular combinations). Other biochemicals than chlorophyll have never been addressed in directional studies and almost all investigations used monodirectional measurements without combining different angular data for analyses.

The unprecedented availability of simultaneously acquired multiangular and hyperspectral observations from space is a prerequisite to systematically assess the benefits of directional information for the estimation of canopy biochemistry. Only canopy reflectance observations in high spectral resolution and from multiple viewing angles, as provided by the spaceborne mission CHRIS/PROBA, allowed us to perform such a study. In this paper we focus on nitrogen concentration (C_N) that is related to the maximum photosynthetic rate [20-23], ecosystem productivity [24], soil respiration and decay rate of leaf litter [25, 26] and thus influence global cycling of carbon. It was shown that spatial estimates of nitrogen concentration are essential to improve the parameterization and results of ecosystem models [27-31]. Knowledge of canopy nitrogen is important for a range of environmental applications [32-34], including invasive species detection [34], desertification mapping [35] and forest health status monitoring. Thus, such estimates carry an important economic component not only regarding forest products [36] but also in terms of protection forests, which protect people and infrastructure against natural hazards [37].

The presented research has examined statistical methods to readily obtain biochemical values from directional data by explicitly using an application-oriented approach. We aimed at showing potential benefits of directional data also for widely used, simple and fast statistical methods since operational techniques largely remain on products derived from empirical studies. Indeed, many uncertainties and errors with which we have to cope in empirical studies could be either addressed implicitly or removed in pure modeling studies.

The objective of this study was to investigate the contribution of directional data for the estimation of C_N by evaluating regression models based on various combinations of CHRIS viewing angles and spectral processing. Specifically, we investigated: a) if the information contained in remotely sensed multiangular data impacts models to estimate C_N, b) if certain sensor viewing angles emerge to be beneficial for estimating C_N, and c) if this information remains after continuum removal and normalization have been applied to reflectance data.

2 DATA ACQUISITION

2.1 Study site

The forest study site Vordemwald, VOR, (7°53’ E, 47°16’N) is located in the Swiss Plateau at an altitude of ~400–600 meters above see level. The forest canopy is composed

of a mixture of needle-leaf and broadleaf species, dominated by European beech (*Fagus sylvatica* L.), European ash (*Fraxinus excelsior* L.), black alder (*Alnus glutinosa* (L.) Gaertn.), silver fir (*Abies alba* Mill.) and Norway spruce (*Picea abies* L.). In total nine different species were sampled belonging to two plant functional types (coniferous-evergreen and broadleaf-deciduous).

Prior to field data sampling, we purposively determined 15 subplots at the study site VOR, each covering roughly an area of 2500 square meters (~3x3 CHRIS pixels). Subplot selection was targeted at gathering high species homogeneity so that all species within a subplot belong to the same plant functional type. In addition, the species had to be dominant within a group of neighboring trees so that all trees within a CHRIS pixel (and its positional uncertainty) were of a similar species and chemistry as the target tree. Next, at each subplot, 3–10 target trees were determined for foliar sampling. Target tree selection was aimed at capturing a broad range of C_N and at minimizing background influences. The latter was achieved by selecting trees with large treetops. Additionally to the target trees, all subsequently described measurements (except of biochemistry estimates) were also determined for all trees growing by the side of target trees.

2.2 Field data sampling

In July 2004, field data were sampled to determine leaf biochemistry in the laboratory and to obtain additional biophysical and positional tree properties. At the 15 subplots of the study site, a tree climber excised leaf samples of three different upper sunlit canopy branches from a total of 60 trees, whereof 33 were conifers and 27 broadleaves. To obtain representative samples, we collected 5 leaves per branch from all selected deciduous trees and 5 needles of the first three age classes per branch from all needle-leaf trees (45 needles per tree). For each sampled (target) tree the collected leaf material was pooled, sealed in bags and stored in a cool box for transportation. Tree heights and crown dimensions were assessed with a Forestor Vertex Hypsometer [38, 39] for all trees. The heights of the target trees ranged from 26 m to 46 m with a mean of 34 m, whereas the mean diameter of a broadleaf and a needle-leaf tree crown was found to be 8.1 m and 6.4 m, respectively. Further, for all trees Diameter at Breast Height (DBH) was measured and the species type noted.

Tree trunk positions were measured using a Trimble GeoXT GPS receiver including correction for multipath biases for subsequent geolocation of the sampled individual tree crowns. We improved the positional accuracy by calculating the mean of 20 to 40 GPS measurements per trunk and by applying a post processing differential correction to the recorded data using the Pathfinder Office software [40]. CHRIS data acquisition was two years after field data collection but during the same phenological period (July). We assumed a stable C_N level [27] during July and only small inter-annual variability for nitrogen concentration [41] due to similar climatic conditions in the years 2004 and 2006 [42]. This assumption was confirmed by repeated leaf sample collections taken on one subplot over 10 years, which belongs to the framework of the IPC Forest monitoring.

2.3 Laboratory analyses and canopy nitrogen content determination

Leaf area, fresh and dry weight, and biochemical composition of all 60 collected leaf samples were determined in the laboratory. An LI-3100 Area Meter [43] was used to obtain the single-sided leaf area of the samples. Fresh and dry mass were determined by weighing the samples before and after being oven-dried at 85° C until a constant weight was achieved. For nitrogen analyses the samples were dried at 65 °C until a constant weight was achieved, then ground to powder and finally a subsample of the powder injected into an elemental analyzer (NA 2500; CE Instruments, Milan, Italy). For each tree, two subsamples were analyzed and checked for within-subsample variation. None of the samples exceeded the threshold of 3 % variation between the two sub-sample measurements and its mean. Finally, plot-level canopy nitrogen concentration (g N per 100 g foliage biomass) for each of the 15 subplots (Table 1) was derived by calculating

the mean of foliar nitrogen concentration for all individual species in the subplot, weighted by the fraction of foliage biomass per species within a subplot [44]. Allometric equations were used to obtain foliage biomass by species [45]. Mass-based nitrogen concentration has been shown to be quite invariable within the vertical canopy [46].

Table 1. Dominant functional type (BD: broadleaf deciduous samples, NE: needle-leaf evergreen samples) and descriptive statistics of biochemical properties by subplot.

Subplot	Functional type	Plot-level canopy nitrogen concentration [g /100 g]
GR1	BD	1.651
GR2	BD	2.354
GR3	NE	1.160
LWF1	NE	1.270
LWF2	NE	1.186
MB1	NE	1.124
MB2	NE	1.204
MB3	NE	1.122
S1	BD	2.136
S2	NE	1.264
S3	BD	2.384
WH1	BD	2.531
WH2	NE	1.360
WM1	BD	2.029
WM2	BD	1.860

2.4 CHRIS data acquisition and processing

The investigations were carried out using mode 5 data of the spaceborne ESA-mission CHRIS (Compact High Resolution Imaging Spectrometer) on-board PROBA-1 [47], which provides multiangular data in the range from 447 nm to 1035 nm in 37 bands with a spatial resolution of 18 m. CHRIS simultaneously supplies five viewing angles with the nominal fly-by zenith angles (FZA's) at ±36°, ±55° and 0° (nadir). The images were acquired on July 1, 2006, over the study site Vordemwald and covered an area of 6.5x13 km.

The actual viewing zenith angles of CHRIS data acquisitions do rarely represent the nominal FZA's due to uncertainties in pointing [48]. As can be seen in Fig. 1a, the actual viewing angle for the nadir image was for instance -7.3° in the backward scattering viewing direction. In addition, the figure shows that the acquisition has not occurred accurately in the solar principal plane where anisotropic effects are most pronounced for vegetation.

The five CHRIS multiangular acquisitions were orthorectified and radiometrically corrected. Geometric correction was based on a 3D physical model [49, 50], which is implemented in the commercially available image processing software PCI/OrthoEngine [51]. The procedure accounts for the real acquisition geometries. High positional accuracy of the respective multiangular products after geometric correction was a prerequisite for a reliable extraction of spectral information from the five images. To achieve a high geometric accuracy and a co-registration of the multiangular image cubes, georegistration was carried out on all five cubes using a digital surface model (DSM) (swisstopo) with 2 m resolution [52]. The resulting RMSEs derived from Ground Control Points (GCP's) were at 0.46–0.79 pixels along track and 0.39–0.73 pixels across track. The co-registration of the angles is illustrated by Fig. 1b. If registration is perfect, a greyscale image is obtained.

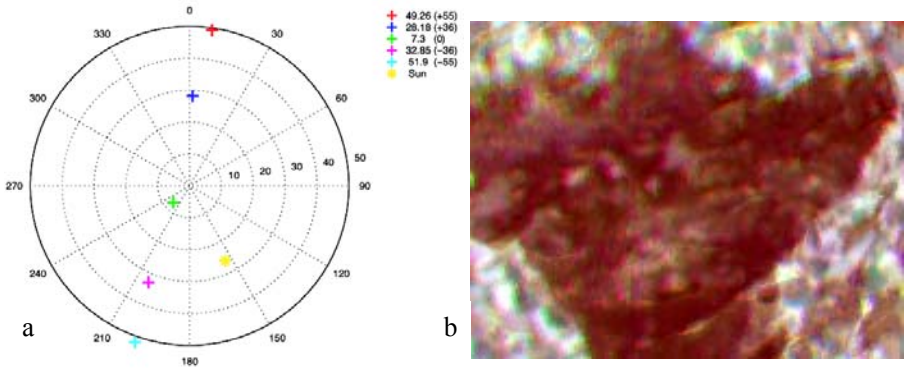

Fig. 1. a) Acquisition geometries and illumination angles for the five CHRIS images acquired on July 1, 2006. The nominal fly-by zenith angles are listed in brackets. The center of the plot represents the target. b) Three angle color composite (nadir (R), +55°(G), -55°(B)@728nm) showing the northern part of the VOR study site.

Subsequent atmospheric correction of the CHRIS radiance data was performed using ATCOR-3 [53], which is based on MODTRAN-4. ATCOR-3 enables the processing of data from tilted sensors by accounting for varying path lengths through the atmosphere, varying transmittance and for terrain effects by incorporating digital terrain model (DTM) data and their derivatives such as slope and aspect, sky view factor and cast shadow. For the atmospheric processing a laser-based DTM with 2 m spatial resolution (swisstopo) was resampled to 18 m using bilinear interpolation [54].

2.5 Subplot spectra extraction and processing

After geometric and atmospheric correction, canopy reflectances corresponding to the 15 subplots with field-sampled tree crowns were extracted from the five CHRIS images thus obtaining a total of five sets each consisting of 15 spectral signatures representing the subplots. The geographical trunk positions (vector data) of the sampled trees were used to define the subplot boarders and to locate the pixels in the images and to extract mean spectral data. Figure 2a illustrates the viewing angle dependant spectral signatures extracted from a co-registered subplot representing a needle-leaf evergreen stand.

3 METHODS

For further analyses four datasets were generated per viewing angle (e.g., nadir). One of the four datasets consisted of original reflectance and the other three of continuum-removed data using different algorithms. The datasets were termed as follows: SPEC represented original reflectance values; BNA represented band depths normalized to the area of the absorption feature, BNC represented band depths normalized to the waveband at the center of the absorption feature and CRDR represented continuum-removed derivative reflectance. The spectral data processing and statistical analysis are described in the following subsections.

3.1 Processing of spectral data

Continuum removal is a normalization technique aimed at enhancing the spectral features of interest while minimizing extraneous factors, such as atmospheric absorptions, anisotropic effects or soil background effects [55]. The observed spectral continuum is considered an estimate of the other absorptions present in the spectrum, not including the one of interest [56]. To approximate the continuum lines, straight-line segments were used that connect local spectra maxima of absorption features in the region of 551–755 nm. The continuum-removed reflectance (R') is calculated by dividing the original

reflectance values by the corresponding values of the continuum line [55]. From the continuum-removed reflectance, the band depth of each point in the absorption feature was computed by subtracting the continuum-removed reflectance from one. To minimize extraneous influences, we applied two normalization procedures on band depths: 1) band depths normalized to the area of the absorption feature (BNA), as proposed by Curran et al., (2001) and 2) band depths normalized to the waveband at the center of the absorption feature (BNC), as proposed by Kokaly and Clark (1999). Additionally, we calculated the continuum-removed derivative reflectance CRDR [57, 58].

The band depth normalized to the area (BNA) measures the depth of the waveband of interest from the continuum line, relative to the area of the absorption feature [59]. BNA was calculated by dividing the band depth by the area of the absorption feature (Eq. 1):

$$\mathrm{BNA} = \left(1 - \left(R/R_i\right)/A\right), \tag{1}$$

where R is the reflectance of the sample at the waveband of interest, R_i is the reflectance of the continuum line at the waveband of interest and A is the area of the absorption feature below the continuum line.

The band depth normalized to the center (BNC) was calculated by dividing the band depth of each band by the band depth at the band center (Eq. 2):

$$\mathrm{BNC} = \left(1 - \left(R/R_i\right) / 1 - \left(R_c/R_{ic}\right)\right), \tag{2}$$

where R is the reflectance of the sample at the waveband of interest, R_i is the reflectance of the continuum line at the waveband of interest, R_c is the reflectance of the sample at the absorption feature center and R_{ic} is the reflectance of the continuum line at the absorption feature center [59]. The band center is the minimum of the continuum-removed absorption feature [55]. The band center was determined for each spectrum separately and could therefore vary between different spectra. The different BNC signatures of a needle-leaf evergreen subplot obtained from five CHRIS viewing angles are illustrated in Fig. 2b.

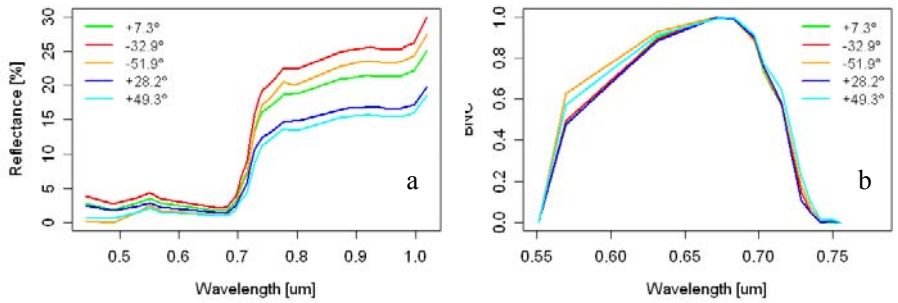

Fig. 2. a) Spectral signatures of the MB1 needle-leaf evergreen stand from processed CHRIS data of the nominal viewing zenith angles at ±36°, ±55° and 0°. Negative viewing zenith angles correspond to the backward scattering direction and positive angles represent the forward scattering direction. b) Band depths normalized to the waveband at the center of the absorption feature (BNC) of the MB1 needle-leaf evergreen subplot for the absorption feature between 551 and 755 nm, from processed CHRIS data of the nominal viewing zenith angles at ±36°, ±55° and 0°.

Continuum-removed derivative reflectance (CRDR) was calculated by applying the first difference transformation described in Eq. 3 to the continuum-removed reflectance spectrum R'.

$$FDR_{\lambda(i)} = \left(R'_{\lambda(j+1)} - R'_{\lambda(j)} \right) \Big/ \Delta_{\lambda} \tag{3}$$

where FDR is the first derivative reflectance at wavelength i situated in the middle between wavebands j and $j + 1$. $R'_{\lambda(j)}$ is the continuum-removed reflectance at waveband j, $R'_{\lambda(j+1)}$ is the continuum-removed reflectance at waveband $j + 1$, and Δ_{λ} is the difference in wavelengths between bands j and $j + 1$ [57, 58].

We applied continuum removal for C_N on the absorption feature located between 551 and 755 nm where the leaf water effect is minimal. Several studies have shown a strong nitrogen-pigment relationship in this region because the chlorophyll content in foliage is highly correlated with total protein and, hence with nitrogen [22, 23, 60, 61]. The reason for this is that proteins are the major nitrogen bearing leaf constituents, typically holding 70–80 % of all nitrogen. An additional 5–10 % of nitrogen is allocated to chlorophyll and lipoproteins [62]. Moreover, the red edge region of the spectrum (680–740 nm) is sensitive to chlorophyll concentration [63-66]. An increase of chlorophyll concentration causes a broadening of the chlorophyll absorption feature centered around 680 nm, resulting in a shift of the point of maximum slope (termed the red edge position) towards longer wavelengths [66]. Finally, reflectance ratios in the red edge did positively correlate with chlorophyll and nitrogen concentrations [65, 67, 68].

3.2 Statistical analyses

Multiple linear regression analysis was applied to fit models between the dependent variable C_N and various viewing angle combinations of the four spectral datasets (SPEC, BNA, BNC and CRDR). To limit the number of spectral wavebands used in the regression models, this study employed a statistical variable selection method, namely an enumerative branch-and-bound (B&B) search procedure [69]. The procedure attempts to evaluate all possible combinations of wavebands for best model fit. Branch-and-bound algorithms are efficient because they avoid exhaustive enumeration by rejecting suboptimal subsets without direct evaluation [70]. The basic characteristics of B&B methods have been addressed by several papers [69-72] and the effectiveness for dimension reduction of hyperspectral data has been demonstrated [73]. We constrained the regression to two selected wavelengths that best explained C_N. We applied this limitation in order to avoid overfitting of the models. The F statistic for all presented models was significant at the 5 % significance level.

An objective of this experiment was to determine whether assessing canopy C_N could be improved with additional directional information. Therefore, we started fitting models on data extracted from one viewing angle only (e.g., nadir). Next, we developed models for all possible combinations of two viewing angles (e.g., nadir and -36°). This resulted in a total of 15 viewing angle combinations, which we evaluated for each spectral dataset. The models were evaluated by comparing the adjusted R^2. The adj. R^2 accounts for the number of predictors and sample points used, which influence the effective degrees of freedom [74]. It does so by lowering the regression R^2 accordingly. Therefore, it is better suited to compare the strengths of model fit that include differing numbers of observations and predictors [74]. To test the models and to assess their predictive capability, we applied a 10-fold cross-validation with random splitting order of the data [73, 75], from which we then calculated the cross-validated RMSE and adj. R^2 (CV RMSE, CV adj. R^2). Cross-validation is an often used procedure, where independent test data is scarce. Due to the comparably low number of sample points involved, we iterated each cross-validation run ten times in order to obtain a more robust cross-validation error

estimate. All analyses were implemented within the R statistical package, a free software environment for statistical computing and graphics [76] under the GNU public license.

4 RESULTS

In total 60 regression models were developed, 15 for each dataset (SPEC, BNA, BNC, CRDR) and 40 of them were developed on data of two observation angles. We added at maximum two independent variables to a model, whenever a second wavelength contributed significantly to the regression fit. This was not the case for 12 models and 7 of them were developed on untransformed spectral data (SPEC). Conversely, with one exception each, all of the BNA and BNC models significantly gained regression fit by adding a second term. Only for 9 models (whereof 5 BNC models), the second significant predictor was from another observation angle than the first one.

4.1 Impact of angular information on canopy nitrogen concentration models

The contribution of angular information to the model fit in terms of adjusted regression R^2 was evaluated among all two-term models. The mean adj. R^2 of all models developed on data of two wavelengths from the same viewing angles was compared with the result of the models developed on data originating from two different angles. The adj. R^2 increased with additional angular information for all datasets (Tab. 2). The highest increase was achieved for the CRDR dataset (+ 87.5 %, compared to the monodirectional two-term models). However, for the SPEC and CRDR datasets, only one out of ten two-angle models effectively contained predictors selected from two different viewing angles.

Table 2. Comparison of mean adjusted R^2 by dataset for two-term models containing either two wavelengths from the same observation angle or from two different viewing angles.

	Mean adj. R^2	
Dataset	2 wavelengths from 1 viewing angle	2 wavelengths from 2 viewing angles
SPEC	0.49	0.78*
BNA	0.51	0.72
BNC	0.47	0.67
CRDR	0.48	0.90*

* value based on only one model.

4.2 Viewing angle combinations for canopy nitrogen concentration estimation

We compared 15 regression models for canopy nitrogen concentration and each dataset to discover the most promising viewing angle combinations for improved estimates of C_N. To assess if directional effects are still present after continuum removal we used four different reflectance datasets (SPEC, BNA, BNC and CRDR). Adj. R^2 values varied considerably in all datasets. For instance they ranged from 0.25 (nadir) to 0.72 (+36°) for C_N single-angle models based on SPEC (Fig. 3). As can be seen from Fig. 3, adj. R^2 values among all spectral datasets and viewing angle combinations followed the same pattern. In case of differences, the SPEC and BNA datasets behaved very similarly as well as the BNC and CRDR datasets. Best performance among different viewing angles was achieved with the BNA and CRDR datasets.

For single angle models, best results were computed for C_N trained on data from the nominal -36° angle for the BNC and CRDR datasets (0.74 and 0.76) and from the nominal -36° angle for the SPEC and BNA datasets (0.72 and 0.75). For the nominal -55° angle, largest adj. R^2 variability among the four different spectral datasets was observed. Poorest results were obtained for regression models developed on nadir and +55° data.

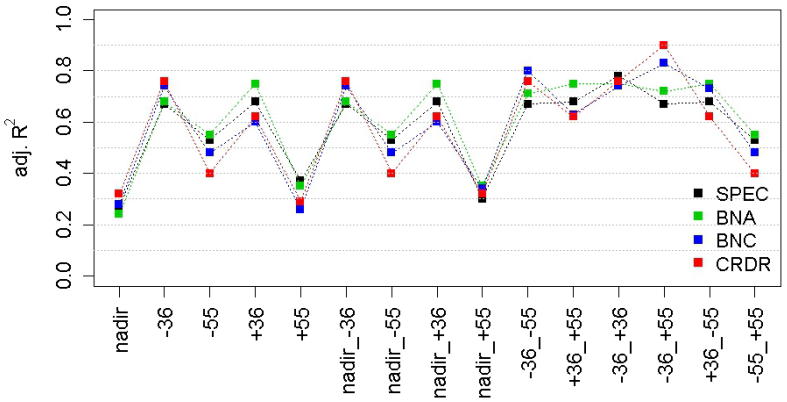

Fig. 3. Adjusted coefficient of determination (adj.R^2) of canopy nitrogen concentration regressed on the datasets SPEC, BNA, BNC and CRDR, respectively.

For two-angle models, the combination of the nadir and +55° angles led to the lowest adj. R^2 values for all datasets and the combination of the -36° and +55° angles for the BNC and CRDR datasets to the highest, demonstrating that simply adding the two best performing angles for monodirectional models does not necessarily lead to the best two-angle model. When adding up the selected wavebands per viewing angle among all 15 models, nadir observations were the least and -36° observations the most selected ones. In terms of selected wavelengths by the B&B subset algorithm, 631.2 nm was selected in 18 %, 682.8, 741.6 and 748.4 nm were selected in about 13 % of all cases.

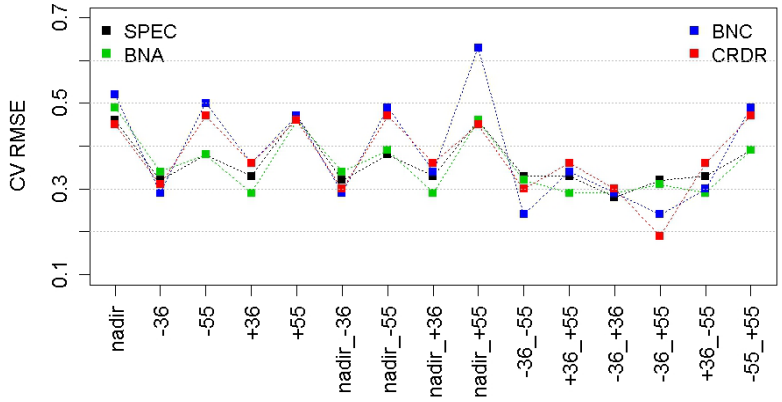

Fig. 4. Cross-validated root mean square error (CV RMSE) of 15 regression models between canopy nitrogen concentration and four spectral datasets (SPEC, BNA, BNC, CRDR). The x-axis shows the evaluated 15 regression models.

The predictive capability of the regression models was evaluated in terms of adj. R^2 and RMSE values of cross-validated models. Figure 4 shows that we obtained the lowest CV-RMSE (0.19) for the CRDR dataset with the wavelength 631.2 nm selected from the -36° and +55° viewing angles. CV-RMSE was more than halved compared to the simple nadir model (CV-RMSE 0.48). Lowest CV RMSE was most often counted for the BNA dataset (6 of 15 cases). The CV RMSE has a smaller variability when based on the SPEC and BNA datasets compared to the BNC and CRDR results.

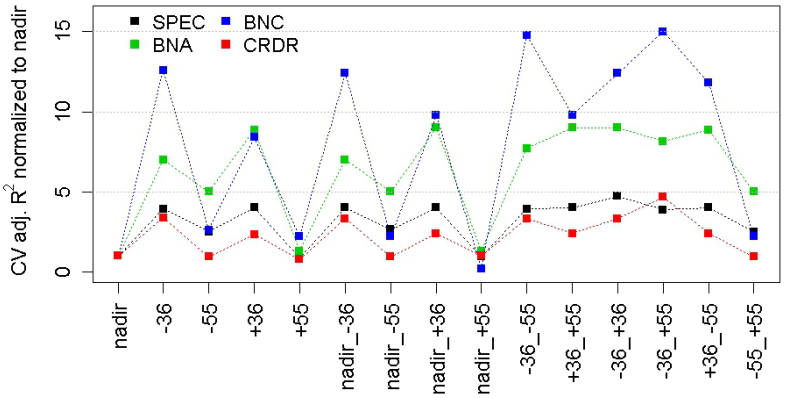

Fig. 5. Cross-validated adj. R^2 of 15 regression models between canopy nitrogen concentration and four spectral datasets (SPEC, BNA, BNC, CRDR) normalized to nadir. The x-axis shows the evaluated 15 regression models.

By normalizing each dataset's cross-validated adj. R^2 values to the value of the nadir model, as depicted by Fig. 5, the improvement of the predictive capability when using off-nadir or combinations of CHRIS angles rather than nadir-only data becomes evident. Most balanced were the SPEC and CRDR models, due to a comparable high adj. R^2 value for the nadir model, whereas BNC models showed largest potential for improvement. For instance, the BNC model developed on data of the -36° and -55° observation angles resulted in a 15 times higher cross-validated adj. R^2 compared to the BNC nadir model.

5 DISCUSSION

In our study, regression results varied considerably among different viewing zenith angles (e.g., C_N regressed on SPEC: adj. R^2 = 0.25–0.78) contradicting the findings of Begiebing and co-workers (2005), who used CHRIS data to retrieve chlorophyll content in crops by radiative transfer inversion. They found only small variation among different angular data [18]. However, only nadir and forward looking angles (+36°, +55°) were discussed without considering backward scattering data and multiangular information (angular combinations).

Yet, the backward scattering direction is of particular interest for vegetation targets. Previous studies found an increase in reflectance for the backward scattering direction in boreal forests but lower reflectance values in the forward scattering direction, due to a combination of gap and backshadow effects [77, 78]. These anisotropic effects are more pronounced at high sun zenith angles and are emphasized in high absorbing spectral ranges (e.g., red band) due to the lack of multiple scattering in this wavelength range [77]. The finding that most information is contained in backward scattering viewing direction reflectance is only partly consistent with our results. We observed that monodirectional models trained on ±36° data generally achieved higher R^2 values and lower model errors than those developed on data of nadir and large zenith angles, even though we also observed increased reflectance for the backscattering directions.

Our research showed that increasing the number of angular information (multiangular) for nitrogen concentration estimation increased regression model fits and lowered cross-validated RMSEs. The findings of this study seem to be consistent with another modeling analysis, albeit performed with synthetic data, which found that best accuracies were obtained with multiple directions to estimate canopy variables [19]. These results indicate that so far the potential of directional data is only partly exploited and that the use of multiangular data, by combining multiple directions, should be augmented for future studies also for application-oriented empirical surveys where fast information is needed.

It has also been shown that the canopy hotspot effect has rich information content for vegetation characterization, especially indications of canopy structure (i.e., a shadow is not visible) [19, 79-81]. In our analysis the viewing zenith angle of -36° is located closest to the images hotspot. Again we point out that CHRIS images were not recorded in the sun principal plane; however, all the monodirectional models developed on this angular data performed about equally well as with forward scattering +36° data, but the variability of the results among all datasets was reduced for -36° data. This is interesting since minimum reflectance values occurred in the forward scattering directions where the sensor views the non-illuminated, shaded leaf surfaces [78]. Our findings revealed in particular poor results for large zenith angles (±55°) when using only one angle, possibly related to uncertainties due to atmospheric correction and shadow effects. But interestingly, overall the best results were achieved with multidirectional models calibrated on -36° (closest to hotspot) and ±55° data. This is in line with Weiss and co-workers findings for chlorophyll content estimation from simulated reflectance data, where mainly off-nadir directions for large zenith angles (and around the hotspot peak) were required [19]. As well [82] report better results for larger observation zenith angles when estimating chlorophyll content. From these viewing angles, the sensor's field of view is still dominated by foliar material and – compared to nadir – the shadows seem to have a lower influence than possible soil background effects. Again in accordance with Weiss et al. (2000) was our finding that for C_N estimates the nadir view direction played a minor role possibly due to shaded background that has strongest influences on the signal for nadir and small off-nadir angles [83]. The large portion of gaps observed in this direction decreases the portion of leaf material seen from the sensor and thus the reflectance values. We are aware that the applied empirical approach neglected radiative transfer processes within the canopy.

To assess possible directional effects in models based on spectrally transformed data we compared the regression results from three continuum-removed datasets (BNA, BNC and CRDR) with those from untransformed reflectance values (SPEC). For single-angle models adj. R^2 values varied considerably between viewing angles, indicating that the normalization procedure was not able to remove extraneous effects and the variability among all datasets was about the same. Even though the best two models in terms of cross-validated RMSE were developed with transformed BNC and CRDR data, the results obtained with SPEC and BNA data were more balanced over different angular combinations.

6 CONCLUSIONS

This study has systematically investigated the contribution of directional CHRIS data to the estimation of canopy C_N by assessing adj. R^2 values and CV-RMSEs of regression model fits between the chemical constituent and 15 angular combinations of four spectral datasets. The goal of the presented research was to show the benefits of directional EO data also for empirical, application-oriented surveys. We found that 1) additional information contained in multiangular data improved regression models fits for canopy C_N estimates and lowered cross-validated RMSEs considerably, 2) the nadir direction alone is not optimal for canopy nitrogen estimation irrespective of data processing, 3) monodirectional models developed on the ±36º viewing directions were generally superior to models based on data of nadir and large zenith angles and 4) best results were achieved with combinations of -36° and ±55°.

Our results suggest that multiangular data improved the prediction of C_N estimates compared to nadir models. This demonstrates that not only the assessment of structural vegetation parameters but also biochemical estimates may profit from additional information contained in multidirectional reflectance data. These findings highlight the potential of multiangular Earth observations for ecological monitoring and modeling studies as already proclaimed by preparatory studies for the ESA Earth Explorer candidate SPECTRA [84] and in addition for application-oriented empirical studies. The relevance of multiangular measurements also to a variety of societal themes has been acknowledged [85].

Acknowledgments

The authors would like to thank the Swiss National Science Foundation (SNF: project no. 200020-101517) for funding this project. Smaller additional funding came from the 5th and 6th Framework Program of the European Union, i.a., the MRTN Hyperspectral Imaging Network (Contract Numbers EVK2-CT-2002-00136, GOCE-CT-2003-505376 and MRTN-CT-2006-035929). The continuing effort and support of ESA and SIRA to provide CHRIS/PROBA data is gratefully acknowledged. We are very grateful to the Swiss Federal Research Institute WSL and the many individuals who have helped with data collection and processing.

References

[1] G. P. Asner, "Biophysical remote sensing signatures of arid and semiarid ecosystems," in *Remote Sensing for Natural Resource Management and Environmental Monitoring*, S.L. Ustin, Ed., pp. 53–109, Wiley, Hoboken, NJ (2004).

[2] M.V. Schönermark, B. Geiger, and H.-P. Röser, *Reflection Properties of Vegetation and Soil : With a BRDF Data Base*, pp. 352 p., Wissenschaft und Technik, Berlin (2004).

[3] M. Minnaert, "The reciprocity principle in lunar photometry," *Astrophys. J.* **93**, 403-410 (1941) [doi:10.1086/144279].

[4] B. Hapke, "Bidirectional reflectance spectroscopy - 1. Theory," *J. Geophys. Res.* **86**(B4), 3039-3054 (1981) [doi:10.1029/JB086iB04p03039].

[5] J. M. Chen, J. Liu, S. G. Leblanc, R. Lacaze, and J.-L. Roujean, "Multi-angular optical remote sensing for assessing vegetation structure and carbon absorption," *Rem. Sens. Environ.* **84**, 516-525 (2003) [doi: 10.1016/S0034-4257(02)00150-5].

[6] M. J. Chopping, A. Rango, K. M. Havstad, F. R. Schiebe, J. C. Ritchie, T. J. Schmugge, A. N. French, L. H. Su, L. McKee, and M. R. Davis, "Canopy attributes of desert grassland and transition communities derived from multiangular airborne imagery," *Rem. Sens. Environ.* **85**, 339-354 (2003) [doi:10.1016/S0034-4257(03)00012-9].

[7] S. Sandmeier and D. W. Deering, "Structure analysis and classification of boreal forests using airborne hyperspectral BRDF data from ASAS," *Rem. Sens. Environ.* **69**, 281-295 (1999) [doi:10.1016/S0034-4257(99)00032-2].

[8] J. L. Widlowski, B. Pinty, N. Gobron, M. M. Verstraete, D. J. Diner, and A. B. Davis, "Canopy structure parameters derived from multi-angular remote sensing data for terrestrial carbon studies," *Climatic Change* **67**, 403-415 (2004) [doi:10.1007/s10584-004-3566-3].

[9] J. Verrelst, M. E. Schaepman, B. Koetz, and M. Kneubuehler, "Angular sensitivity analysis of vegetation indices derived from CHRIS/PROBA data," *Rem. Sens. Environ.* **112**, 2341-2353 (2008) [doi:10.1016/j.rse.2007.11.001].

[10] D. J. Diner, G. P. Asner, R. Davies, Y. Knyazikhin, J. P. Muller, A. W. Nolin, B. Pinty, C. B. Schaaf, and J. Stroeve, "New directions in earth observing: Scientific applications of multiangle remote sensing," *Bull. Am. Meteorol. Soc.* **80**, 2209-2228 (1999) [doi: 10.1175/1520-0477(1999)080<2209:NDIEOS>2.0.CO;2].

[11] S. L. Ustin, P. J. Zarco-Tejada, S. Jacquemoud, and G. P. Asner, "Remote sensing of the environment: state of the science and new directions," in *Remote Sensing for Natural Resource Management and Environmental Monitoring*, S. L. Ustin, Ed., pp. 679–729, Wiley, Hoboken, NJ (2004).

[12] J. Heiskanen, "Tree cover and height estimation in the Fennoscandian tundra-taiga transition zone using multiangular MISR data," *Rem. Sens. Environ.***103**, 97-114 (2006) [doi: 10.1016/j.rse.2006.03.015].

[13] D. S. Kimes, K. J. Ranson, G. Sun, and J. B. Blair, "Predicting lidar measured forest vertical structure from multi-angle spectral data," *Rem. Sens. Environ.***100**, 503-511 (2006) [doi:10.1016/j.rse.2005.11.004].

[14] S. Begiebing, H. Bach, and W. Mauser, "Assimilation of hyperspectral multi-directional CHRIS-data in a coupled radiative transfer and crop growth model," *Proc. Envisat Symp.*, **ESA SP-636** (2007).

[15] M. J. Barnsley, D. Allison, and P. Lewis, "On the information content of multiple view angle (MVA) images," *Int. J. Rem. Sens.* **18**, 1937-1960 (1997) [doi:10.1080/014311697217963].

[16] E. C. Brown de Colstoun and C. L. Walthall, "Improving global scale land cover classifications with multi-directional POLDER data and a decision tree classifier," *Rem. Sens. Environ.***100**, 474-485 (2006) [doi: 10.1016/j.rse.2005.11.003].

[17] N. Gobron, B. Pinty, M. M. Verstraete, J. V. Martonchik, Y. Knyazikhin, and D. J. Diner, "Potential of multiangular spectral measurements to characterize land surfaces: conceptual approach and exploratory application," *J. Geophys. Res.-Atmosph.* **105**, 17539-17549 (2000) [doi: 10.1029/2000JD900154].

[18] S. Begiebing, H. Bach, D. Waldmann, and W. Mauser, "Analyses of spaceborne hyperspectral and directional CHRIS data to deliver crop status for precision agriculture," *Proc. 5th European Conf. Precision Agricult.* (2005) http://www.preagro.de/Veroeff/ECPA05_VISTA.pdf.

[19] M. Weiss, F. Baret, R. B. Myneni, A. Pragnere, and Y. Knyazikhin, "Investigation of a model inversion technique to estimate canopy biophysical variables from spectral and directional reflectance data," *Agronomie* **20**, 3-22 (2000) [doi:10.1051/agro:2000105].

[20] R. S. Dubey, "Handbook of photosynthesis," in *Books in Soils, Plants, and the Environment*, M. Pessarakli, Ed., pp. 717–737, Taylor & Francis, Boca Raton, FL (2005).

[21] P. B. Reich, B. D. Kloeppel, D. S. Ellsworth, and M. B. Walters, "Different photosynthesis-nitrogen relations in deciduous hardwood and evergreen coniferous tree species," *Oecologia* **104**, 24-30 (1995) [doi:10.1007/BF00365558].

[22] C. Field and H. A. Mooney, "The photosynthesis–nitrogen relationship in wild plants," *On the Economy of Plant Form and Function : Proceedings of the Sixth Maria Moors Cabot Symposium, Evolutionary Constraints on Primary Productivity, Adaptive Patterns of Energy Capture in Plants, Harvard Forest***,** 25–55 (1986).

[23] J. R. Evans, "Photosynthesis and nitrogen relationships in leaves of C_3 plants," *Oecologia* **78**, 9-19 (1989) [doi: 10.1007/BF00377192].

[24] M.-L. Smith, S. V. Ollinger, M. E. Martin, J. D. Aber, R. A. Hallett, and C. L. Goodale, "Direct estimation of aboveground forest productivity through hyperspectral remote sensing of canopy nitrogen," *Ecolog. Applicat.* **12**, 1286-1302 (2002) [doi: 10.1890/1051-0761(2002)012[1286:DEOAFP]2.0.CO;2].

[25] W. Merrill and E. B. Cowling, "Role of nitrogen in wood deterioration - amounts and distribution of nitrogen in tree stems," *Can. J. Botany* **44**, 1555-1580 (1966) [doi: 10.1139/b66-168].

[26] J. M. Melillo, J. D. Aber, and J. F. Muratore, "Nitrogen and lignin control of hardwood leaf litter decomposition dynamics," *Ecol.* **63**, 621-626 (1982) [doi: 10.2307/1936780].

[27] M. E. Martin and J. D. Aber, "High spectral resolution remote sensing of forest canopy lignin, nitrogen, and ecosystem processes," *Ecolog.l Applicat.***7**, 431-443 (1997) [doi: 10.2307/2269510].

[28] Y. D. Pan, J. Horn, J. Jenkins, and R. Birdsey, "Importance of foliar nitrogen concentration to predict forest productivity in the Mid-Atlantic region," *Forest Sci.* **50**, 279-289 (2004).

[29] D. P. Turner, M. Guzy, M. A. Lefsky, W. D. Ritts, S. Van Tuyl, and B. E. Law, "Monitoring forest carbon sequestration with remote sensing and carbon cycle modeling," *Environment. Manage.* **33**, 457-466 (2004) [doi: 10.1007/s00267-003-9103-8].

[30] A. Psomas, M. Kneubuehler, S. Huber, K. Itten, and N. E. Zimmermann, "Coupling imaging spectroscopy and ecosystem process modelling -the importance of spatially distributed foliar biochemical concentration estimates for modelling NPP of grassland habitats," *IEEE Int. Geosci. Rem. Sens. Symp.* **2**, 315-318 (2008) [doi: 10.1109/IGARSS.2008.4778991].

[31] S.V. Ollinger and M. L. Smith, "Net primary production and canopy nitrogen in a temperate forest landscape: an analysis using imaging spectroscopy, modeling and field data," *Ecosyst.* **8**, 760-778 (2005) [doi: 10.1007/s10021-005-0079-5].

[32] S. L. Ustin, D. A. Roberts, J. A. Gamon, G. P. Asner, and R. O. Green, "Using imaging spectroscopy to study ecosystem processes and properties," *Biosci.* **54**, 523-534 (2004) [doi: 10.1641/0006-3568(2004)054[0523:UISTSE]2.0.CO;2].

[33] P.J. Curran, "Imaging spectrometry for ecological applications," *Int. J. Appl. Earth Observat. Geoinfo.* **3**, 305-312 (2001) [doi: 10.1016/S0303-2434(01)85037-6].

[34] G. P. Asner and P. M. Vitousek, "Remote analysis of biological invasion and biogeochemical change," *PNAS* **102**, 4383-4386 (2005) [doi:10.1073/pnas.0500823102].

[35] G. P. Asner, C. E. Borghi, and R. A. Ojeda, "Desertification in central Argentina: changes in ecosystem carbon and nitrogen from imaging spectroscopy," *Ecolog. Applicat.* **13**, 629-648 (2003) [doi: 10.1890/1051-0761(2003)013[0629:DICACI]2.0.CO;2].

[36] D. G. Goodenough, J. Pearlman, H. Chen, A. Dyk, T. Han, J. Li, J. R. Miller, and O. K. Niemann, "Forest information from hyperspectral sensing," *IEEE Int. Geosci. Rem. Sens. Symp.*, **4,** 2585–2589 (2004).

[37] P. Brang, W. Schönenberger, E. Ott, and B. Gardner, "Forests as protection from natural hazards," in *The Forests Handbook*, J. Evans, Ed., pp. 53–81, Blackwell Science, Oxford Malden, MA (2001).

[38] Haglof Inc., *http://www.haglofsweden.com,* accessed 16 Jan. 2007.

[39] H. Kramer and A. Akça, *Leitfaden zur Waldmesslehre*, J. D. Sauerländer's, Frankfurt am Main, Germany (1995).

[40] Trimble, *GPS Pathfinder Office Software V3.10* (2005).

[41] G. Grassi, E. Vicinelli, F. Ponti, L. Cantoni, and F. Magnani, "Seasonal and interannual variability of photosynthetic capacity in relation to leaf nitrogen in a deciduous forest plantation in northern Italy," *Tree Physiol.* **25**, 349-360 (2005) [doi:10.1093/treephys/25.3.349].

[42] Swiss Federal Office of Meteorology and Climatology MeteoSchweiz, *http://www.meteoschweiz.admin.ch/web/en/climate/climate_today.html,* accessed Feb. 2010 (2006).

[43] LI-COR, *LI-3100 Area Meter Instruction Manual*, LI-COR: Lincoln, NE (1987).

[44] M.-L. Smith and M. E. Martin, "A plot-based method for rapid estimation of forest canopy chemistry," *Can. J. Forest Res.-Revue Can. De Rech. Forestiere* **31**, 549-555 (2001) [doi: 10.1139/cjfr-31-3-549].

[45] D. Perruchoud, F. Kienast, E. Kaufmann, and O. U. Braker, "20th century carbon budget of forest soils in the Alps," *Ecosyst.* **2**, 320-337 (1999) [doi:10.1007/s100219900083].

[46] A. L. O'Neill, J. A. Kupiec, and P. J. Curran, "Biochemical and reflectance variation throughout a Sitka spruce canopy," *Rem. Sens. Environ.***80**, 134-142 (2002) [doi: 10.1016/S0034-4257(01)00294-2].

[47] M. J. Barnsley, J. J. Settle, M. A. Cutter, D. R. Lobb, and F. Teston, "The PROBA/CHRIS mission: a low-cost smallsat for hyperspectral multiangle observations of the Earth surface and atmosphere," *IEEE Trans. Geosci. Rem. Sens.* **42**, 1512-1520 (2004) [doi: 10.1109/TGRS.2004.827260].

[48] M. Davidson and P. Vuilleumier, *Note on CHRIS Acquisition Procedure and Image Geometry; http://earth.esa.int/pub/ESA_DOC/CHRIS_acquisition-procedure_image-geometry_rev1_3.pdf (accessed March 2010),* 2005.
[49] T. Toutin, "Review article: geometric processing of remote sensing images: models, algorithms and methods," *Int. J. Rem. Sens.* **25**, 1893-1924 (2004) [doi: 10.1080/0143116031000101611].
[50] M. Kneubühler, B. Koetz, S. Huber, N. Zimmermann, and M. Schaepman, "Space-based spectro-directional measurements for the improved estimation of ecosystem variables," *Can. J. Rem. Sens.* **34**, 192-205 (2008).
[51] PCI Geomatics, *OrthoEngine, User's Guide Version 10.0* (2006).
[52] D. Schläpfer, B. Koetz, S. Gruber, and F. Morsdorf, "The influence of DEM characteristics on preprocessing of DAIS/ROSIS data in high altitude alpine terrain," *Proc. 3rd EARSeL Work. Imaging Spectrosc.***,** 133-139 (2003).
[53] R. Richter, "Correction of satellite images over mountainous terrain," *Appl. Opt.* **37**, 4004–4015 (1998) [doi:10.1364/AO.37.004004].
[54] D. Schläpfer, J. Nieke, and K. I. Itten, "Spatial PSF nonuniformity effects in airborne pushbroom imaging spectrometry data," *IEEE Trans. Geosci. Rem. Sens.* **45**, 458-468 (2007) [doi:10.1109/TGRS.2006.886182].
[55] R. F. Kokaly and R. N. Clark, "Spectroscopic determination of leaf biochemistry using band-depth analysis of absorption features and stepwise multiple linear regression," *Rem. Sens. Environ.* **67**, 267-287 (1999) [doi:10.1016/S0034-4257(98)00084-4].
[56] R. N. Clark and T. L. Roush, "Reflectance spectroscopy: quantitative analysis techniques for remote sensing applications," *J. Geophys. Res.* **89**, 6329-6340 (1984) [doi:10.1029/JB089iB07p06329].
[57] O. Mutanga, A. K. Skidmore, and H. H. T. Prins, "Predicting *in situ* pasture quality in the Kruger National Park, South Africa, using continuum-removed absorption features," *Rem. Sens. Environ.* **89**, 393-408 (2004) [doi:10.1016/j.rse.2003.11.001].
[58] F. Tsai and W. Philpot, "Derivative analysis of hyperspectral data," *Rem. Sens. Environ.* **66**, 41-51 (1998) [doi: 10.1016/S0034-4257(98)00032-7].
[59] P. J. Curran, J. L. Dungan, and D. L. Peterson, "Estimating the foliar biochemical concentration of leaves with reflectance spectrometry testing the Kokaly and Clark methodologies," *Rem. Sens. Environ.***76**, 349-359 (2001) [doi: 10.1016/S0034-4257(01)00182-1].
[60] L. F. Johnson and C. R. Billow, "Spectrometric estimation of total nitrogen concentration in Douglas-fir foliage," *Int. J. Rem. Sens.* **17**, 489-500 (1996) [doi:10.1080/01431169608949022].
[61] B. J. Yoder and R. E. Pettigrew-Crosby, "Predicting nitrogen and chlorophyll content and concentrations from reflectance spectra (400-2500nm) at leaf and canopy scales," *Rem. Sens. Environ.* **53**, 199-211 (1995) [doi: 10.1016/0034-4257(95)00135-N].
[62] F. S. Chapin and R. A. Kedrowski, "Seasonal changes in nitrogen and phosphorus fractions and autumn retranslocation in evergreen and deciduous Taiga trees," *Ecol.* **64**, 376-391 (1983) [doi:10.2307/1937083].
[63] D. N. H. Horler, M. Dockray, J. Barber, and A. R. Barringer, "Red edge measurements for remotely sensing plant chlorophyll content," *Adv. Space Res.* **3**, 273-277 (1983) [doi: 10.1016/0273-1177(83)90130-8].
[64] B. N. Rock, T. Hoshizaki, and J. R. Miller, "Comparison of *in situ* and airborne spectral measurements of the blue shift associated with forest decline," *Rem. Sens. Environ.***24**, 109-127 (1988) [doi:10.1016/0034-4257(88)90008-9].
[65] D. M. Moss and B. N. Rock, "Analysis of red edge spectral characteristics and total chlorophyll values for red spruce (Picea Rubens) branch segments from Mt. Moosilauke, NH, USA," *IEEE Geosci. Rem. Sens. Symp.* **3,** 1529-1532 (1991).
[66] D. M. Gates, H. J. Gates, J. C. Gates, and V. R. Gates, "Spectral properties of plants," *Appl. Opt.* **4**, 11-20 (1965) [doi:10.1364/AO.4.000011].

[67] A. A. Gitelson, M. N. Merzlyak, and H. K. Lichtenthaler, "Detection of red edge position and chlorophyll content by reflectance measurements near 700 nm," *J. Plant Physiol.* **148**, 501-508 (1996) [doi: 10.1016/S0273-1177(97)01133-2].

[68] D. A. Sims and J. A. Gamon, "Relationships between leaf pigment content and spectral reflectance across a wide range of species, leaf structures and developmental stages," *Rem. Sens. Environ.***81**, 337-354 (2002) [doi: 10.1016/S0034-4257(02)00010-X].

[69] A. J. Miller, *Subset Selection in Regression*, pp. xvii, Chapman & Hall/CRC, Boca Raton, FL (2002).

[70] P. M. Narendra and K. Fukunaga, "Branch and bound algorithm for feature subset selection," *IEEE Trans. Comput.* **26**, 917-922 (1977) [doi:10.1109/TC.1977.1674939].

[71] G. M. Furnival and R. W. Wilson, "Regressions by leaps and bounds," *Technomet.* **16**, 499-511 (1974) [doi: 10.2307/1267601].

[72] L. G. Mitten, "Branch-and-bound methods - general formulation and properties," *Operat. Res.***18**, 24-34 (1970) [doi: 10.1287/opre.18.1.24].

[73] S. Huber, M. Kneubuhler, A. Psomas, K. Itten, and N. E. Zimmermann, "Estimating foliar biochemistry from hyperspectral data in mixed forest canopy," *Forest Ecol. Manage.* **256**, 491-501 (2008) [doi: 10.1016/j.foreco.2008.05.011].

[74] S. Weisberg, *Applied Linear Regression*, pp. xii, Wiley, New York (1980).

[75] T. Hastie, R. Tibshirani, and J. Friedman, *The Elements of Statistical Learning: Data mining, Inference, and Prediction*, pp. 533, Springer, New York (2001).

[76] R Development Core Team, "R: A language and environment for statistical computing," R Foundation for Statistical Computing(2005).

[77] D. W. Deering, T. F. Eck, and B. Banerjee, "Characterization of the reflectance anisotropy of three boreal forest canopies in spring-summer," *Rem. Sens. Environ.* **67**, 205-229 (1999) [doi: 10.1016/S0034-4257(98)00087-X].

[78] S. Sandmeier, C. Muller, B. Hosgood, and G. Andreoli, "Physical mechanisms in hyperspectral BRDF data of grass and watercress," *Rem. Sens. Environ.* **66**, 222-233 (1998) [doi:10.1016/S0034-4257(98)00060-1].

[79] S. A. W. Gerstl, "Building a global hotspot ecology with Triana data," *Proc. Rem. Sens. Earth Sci. Ocean, Sea Ice Applicat.*, **3868,** 184-194 (1999).

[80] R. Lacaze, J. M. Chen, J. L. Roujean, and S. G. Leblanc, "Retrieval of vegetation clumping index using hot spot signatures measured by POLDER instrument," *Rem. Sens. Environ.***79**, 84-95 (2002) [doi:10.1016/S0034-4257(01)00241-3].

[81] F. Camacho-de Coca, M. A. Gilabert, and J. Melia, "Hot spot signature dynamics in vegetation canopies with varying LAI," *Proc. Phys. Measure. Signat. Rem. Sens.***,** 303-308 (2001).

[82] S. Stagakis, N. Markos, O. Sykioti, and A. Kyparissis, "Monitoring canopy biophysical and biochemical parameters in ecosystem scale using satellite hyperspectral imagery: an application on a Phlomis fruticosa Mediterranean ecosystem using multiangular CHRIS/PROBA observations," *Rem. Sens. Environ.* **114**, 977-994 (2010) [doi:10.1016/j.rse.2009.12.006].

[83] W. Ni, C. E. Woodcock, and D. L. B. Jupp, "Variance in bidirectional reflectance over discontinuous plant canopies," *Rem. Sens. Environ.***69**, 1-15 (1999) [doi:10.1016/S0034-4257(98)00125-4].

[84] M. Rast, *SPECTRA - Surface Processes and Ecosystem Changes Through Response Analysis*, pp. 74, ESA Publication Division: ESTEC, Nordwijk, the Netherlands (2004).

[85] M. K. Macauley and D. J. Diner, "Ascribing societal benefit to applied remote sensing data products: an examination of methodologies based on the multi-angle imaging spectroradiometer experience," *J. Appl. Rem. Sens.* **1**, 1-20 (2007) [doi:10.1117/1.2799981].

Silvia Huber studied agro-ecology at the Swiss Federal Institute of Technology (ETH) and geography at the University of Zurich, Switzerland. In 2008 she concluded her Ph.D. at the Remote Sensing Laboratories (RSL) of the University of Zurich and worked afterwards for one year as an experienced researcher within the FP6 Marie Curie Research Training Network HYPER-I-NET at Wageningen University, The Netherlands. Currently she is with the Department of Geography and Geology at the University of Copenhagen, Denmark, working on Earth Observation-based vegetation monitoring of the African continent.

Benjamin Koetz received the M.S. degree in Environmental Sciences with a major in Remote Sensing in 2001 from the University of Trier, Germany in collaboration with INRA, France. In 2006 he concluded his Ph.D. studies at the Remote Sensing Laboratories, University of Zurich, Switzerland. Currently he holds a position as Earth Observation (EO) engineer in the Exploitation and Service Division at the European Space Agency, Italy. His scientific expertise focuses on the development of physically-based methodologies to derive geo biophysical EO products relevant for applications such as wildland fires, forestry and agriculture.

Achilleas Psomas received a B.Sc and M.Sc degree in forestry and environmental sciences from the Aristotel University of Thessaloniki, Greece in 2001 and an M.Sc degree in Geographical Information Systems and Remote Sensing from the Wageningen University, The Netherlands in 2003. In 2008 he concluded his Ph.D. studies at the Swiss Federal Research Institute WSL, Birmensdorf and RSL, University of Zurich, Switzerland. The Ph.D. project focused on coupling plant biochemistry parameter derived from hyperspectral remote sensing data with ecosystem process models. He is currently working as a postodoc in ecological remote sensing at WSL.

Mathias Kneubuehler received the M.Sc. degree in geography and the Ph.D. degree in remote sensing with emphasis on spectral assessment of crop phenology, from the University of Zurich in 1996 and 2002, respectively. He is currently the head of the Spectroscopy Laboratory of the Remote Sensing Laboratories, University of Zurich. He is particularly interested in spectrodirectional data analysis and spectral assessment of phenological processes in vegetation. He is experienced in organizing and coordinating ground measurement campaigns and field experiments in the line of spectrodirectional data acquisition and vicarious calibration.

Jürg T. Schopfer studied geophysics at the ETH Zurich and geography at the Universities of Berne and Zurich, Switzerland, where he received the M.Sc. and Ph.D degrees in 2004 and 2008, respectively. His interests as a Research Scientist at the RSL included spectrodirectional research in EO, spectrodirectional measurment systems and its application, as well as imaging spectroscopy. Currently, he is working as Scientific Advisor for Earth Observation and Security Programmes at the Swiss Space Office (SSO) and is Swiss Delegate to ESA.

Klaus I. Itten received the M.Sc. and Ph.D. degrees in geography from the University of Zurich, Switzerland, in 1969 and 1973, respectively. Since 1982, he has been a Professor in geography and remote sensing at the University of Zurich. As head of the Remote Sensing Laboratories, his research and teaching interests were remote sensing and image processing for natural resources inventorying and monitoring. Imaging spectroscopy and spectroradiometry became important parts of his endeavours. In March 2009 he retired.

Niklaus E. Zimmermann is a research ecologis at the Swiss Federal Research Institute WSL, Birmensdorf, Switzerland. He has received the M.S. degree in plant ecology and a Ph.D. degree in ecological modeling at the University of Berne, Switzerland. He is focusing on spatial ecology, ecological modeling, and environmental remote sensing. Currently, he is head of the Land Use Dynamics research unit at WSL.

Journal of Applied Remote Sensing

Impact of multiangular information on empirical models to estimate canopy nitrogen concentration in mixed forest

Silvia Huber
Benjamin Koetz
Achilleas Psomas
Mathias Kneubuehler
Jürg T. Schopfer
Klaus I. Itten
Niklaus E. Zimmermann